WARWICK
THE UNIVERSITY OF WARWICK

Manuscript version: Author's Accepted Manuscript
The version presented in WRAP is the author's accepted manuscript and may differ from the published version or Version of Record.

Persistent WRAP URL:
http://wrap.warwick.ac.uk/163563

How to cite:
Please refer to published version for the most recent bibliographic citation information. If a published version is known of, the repository item page linked to above, will contain details on accessing it.

Copyright and reuse:
The Warwick Research Archive Portal (WRAP) makes this work by researchers of the University of Warwick available open access under the following conditions.

Copyright © and all moral rights to the version of the paper presented here belong to the individual author(s) and/or other copyright owners. To the extent reasonable and practicable the material made available in WRAP has been checked for eligibility before being made available.

Copies of full items can be used for personal research or study, educational, or not-for-profit purposes without prior permission or charge. Provided that the authors, title and full bibliographic details are credited, a hyperlink and/or URL is given for the original metadata page and the content is not changed in any way.

Publisher's statement:
Please refer to the repository item page, publisher's statement section, for further information.

For more information, please contact the WRAP Team at: wrap@warwick.ac.uk.

warwick.ac.uk/lib-publications

Deep Learning Based Detection for Communications Systems with Radar Interference

Chenguang Liu, Yunfei Chen, *Senior Member, IEEE*, Shuang-Hua Yang, *Senior Member, IEEE*

***Abstract*—Due to the increasing demand for spectrum resources, the co-existence of communications and radar systems has been proposed that allows radar and communications systems to operate in the same frequency band. On the other hand, deep learning has shown great potential in revolutionizing communications systems. In this work, we investigate the use of deep learning in communications systems subject to interference from radar systems. Specifically, we consider a single-carrier communications system. Linear frequency-modulated (LFM) and frequency-modulated continuous-wave (FMCW) are considered for radar. Several important system parameters, including the level of noise and interference, the radar interference coverage, the symbol duration, feature extraction methods and the number of hidden layers are investigated for the performance of the detector. Fully connected deep neural network (FCDNN) and long short-term memory (LSTM) detectors are implemented, where principle component analysis (PCA) is applied to preprocess the observed signals for the FCDNN detector. Numerical results show that the learning-based detector achieves comparable performance in the radar-communication system to the traditional detector but without interference cancellation. Preprocessing the received signals with PCA can improve the performance of FCDNN when interference is strong. Also, LSTM shows more robust performance than FCDNN when the channel has time-related distortion.**

***Index Terms*—Communications, deep learning, radar interference, signal detection.**

I. Introduction

DUE to the increasing demand for wireless communications services, spectrum resources have become scarce. The carrier frequency for wireless communications has been moving towards the radar bands, as the utilization of radar has been extended to civil applications, such as traffic control and vehicle cruise. To improve spectrum efficiency, several researches have been conducted on the co-existence of communications and radar systems in different fields, such as waveform design [1] [2] [3] [4], interference mitigation [5] [6] [7], spatial separation [8], communication receiver design [9] and joint radar and communication systems [10] [11] [12] [13].

One solution to the co-existence of radar and communications is to cooperatively manage the spectrum resources via coordination to allow each system to operate efficiently. The work in [8] proposed a carrier aggregation resource allocation algorithm to manage the band allocation for the co-existence of LTE advanced cellular and S-band radar. The works in [2] [3] [4] proposed the transmit waveform designs to guarantee the performance of the dual-functional radar-communication system, whereas the work in [14] utilized the spectrum sensing techniques from cognitive radio for waveform and receiver design in the radar-communication system. Unlike the works in [2], [3], [4], [8] and [14] with only one active transmitter in the co-existence system, co-design (or joint-design) for both radar waveform and communication system was proposed in [10]- [11] [12] [13], which allows both systems to transmit simultaneously. The work in [10] concluded that co-design plays an important role in performance optimization in co-existence. In [11], a joint radar-communication framework was proposed to enable both systems to operate at the same time with only one transmitted signal. The work in [12] proposed a sharing and allocation-based joint-design for multi-carrier waveforms in radar and communication systems, while the work in [13] proposed a spectrum sharing scheme for the co-existence between MIMO communication system and surveillance radar.

Another solution to the co-existence of radar and communications is to allow radar and communications systems to operate over the same frequency and time. This leads to mutual interference, and one has to modify one of the systems to account for interference. The work in [6] implemented an iterative joint interference elimination process at the communications receiver by exploiting the structure of the radar interferences in an uncoordinated scenario where a communication receiver operated in the presence of radar. The work in [7] proposed a novel beamforming algorithm for MIMO radar and communication to save transmission power by interference mitigation. All the aforementioned works have provided useful results to improve spectrum efficiency, mitigate mutual interference or manage spectrum cooperatively. However, sophisticated redesign and cooperation at transmitter and receiver are often required at the radar or communication systems, which dramatically increases the complexity of these systems.

Signal detection plays a significant role by determining the desired data from a set of noisy and interfered signals collected at receiver. The traditional signal detectors, such

Copyright (c) 2015 IEEE. Personal use of this material is permitted. However, permission to use this material for any other purposes must be obtained from the IEEE by sending a request to pubs-permissions@ieee.org.

This research is supported by the National Natural Science Foundation of China under Grant (61873119 and 92067109), the National Key R&D Program of China under Grant No. 2019YFC0810705 and the Science and Technology Innovation Commission of Shenzhen under Grant No. KQJSCX20180322151418232. (*Corresponding author: Shuang-Hua Yang.)*

Chenguang Liu is with the School of Engineering, University of Warwick, Coventry, UK, CV4 7AL (e-mail: Chenguang.Liu@warwick.ac.uk).

Yunfei Chen is with the School of Engineering, University of Warwick, Coventry, UK, CV4 7AL (e-mail: Yunfei.Chen@warwick.ac.uk).

Shuang-Hua Yang is with the Department of Computer Science and Engineering, Southern University of Science and Technology (SUSTech), Shenzhen, China (e-mail: yangsh@sustech.edu.cn).

as maximum likelihood detectors and zero-forcing forcing detectors, highly depend on the channel state information. The estimation of channel state information introduces extra costs for detection. Also, the accuracy of signal detection is affected by the channel estimation error. On the other hand, deep neural networks have been successfully applied in many research areas, including computer vision [15] and natural language processing [16] due to their powerful capability of recognizing patterns directly from raw data. Therefore, many works have been conducted to apply deep learning to signal detection in communications system without channel estimation.

Some representative works on deep learning in communications signal detection are summarized in [17] and [18]. The work in [19] proposed a learning-based signal detector, DetNet, for MIMO communication, while convolutional neural network and recurrent neural network were applied in [20] to detect signals in MIMO communications system assuming perfect channel estimation. The work in [21] proposed to apply a fully connected neural network to estimate channel state information implicitly to recover the transmitted signals. It showed that deep neural network has advantages in wireless channels with severe distortion and interference. The work in [22] proposed a sliding bidirectional recurrent neural network for sequential signal detection, which outperformed a Viterbi detector with imperfect channel state information and showed robustness in fast-changing channels. The work in [23] proposed ViterbiNet as an ML-based symbol detector incorporating deep neural networks into the Viterbi algorithm. ViterbiNet outperformed previously proposed ML-based detectors and showed the capability of operating under uncertain channel state information and complex channel models. The work in [24] integrated deep neural network into orthogonal approximate message passing algorithm for MIMO detection. Furthermore, the method was improved in [25] by considering imperfect channel state information and adapting various channel environments. In [26], a parallel detection network was proposed to solve the problem that increasing the number of network layers cannot improve the system performance. The work in [27] evaluated the system performance of signal detection in the presence of co-channel interference and proved that the learning-based detectors can perform better than traditional detectors. These works have demonstrated that the learning-based signal detector can achieve good performance in the communications system under various channel conditions.

Although the above studies have elucidated how radar and communications systems can coexist with acceptable performance deterioration and how the communications systems can benefit from deep learning, to the best of the authors' knowledge, there has been no existing work on the use of deep learning in signal detection for communications systems in the presence of radar interference. In this paper, our research focuses on the application of deep learning to a single-carrier communications system in the presence of radar interference. The main contributions of this paper are summarized as below:

1) We analyze the detection performance with respect to different modulations, interference coverage, symbol durations, signal-to-interference ratios (SIRs) and signal-to-noise ratios (SNRs). We also discuss the effect of the number of layers and features on the fully connected deep neural network (FCDNN) detector.
2) Unlike most existing works which improve the radar-communication system by using sophisticated waveform design, interference mitigation or coordination algorithms, we directly use deep neural networks as the signal detector in communications system without estimating the channel or waveform designs.
3) Both symbol-by-symbol detector FCDNN and sequence detector LSTM are implemented. From the numerical results, the learning-based detectors FCDNN and LSTM have considerable accuracy in the radar-communication system compared with the zero-forcing detector with the least-squares channel estimator. Additionally, principal component analysis (PCA) as the preprocessing algorithm can improve the performance of FCDNN when SIR is below 15 dB. Furthermore, LSTM shows more robustness than FCDNN when the channel has time-related distortion. Also, higher interference coverage can degrade the system more than higher peak amplitude of the radar interference for the same SIR condition. FCDNN over ten layers can cause overfitting and compromise the system performance.

The rest of the paper is organized as follows. In Section II, we will introduce the radar-communication system model. Section III discusses the deep learning-based detection, radar interference in communications systems and the data preprocessing methods. Simulation settings will be discussed in Section IV. Simulation results will be presented in Section V. Finally, Section VI will conclude the work.

II. System Model

Consider a narrow-band radar interference in a single-input single-output communications system. The received discrete complex-valued baseband equivalent signal can be expressed as

$$y = hx + mr + n, \tag{1}$$

where h and m are the communications channel gain and radar-to-communications channel gain following Gaussian distributions, respectively, n denotes the additive white Gaussian noise with mean zero and variance σ^2, x denotes the transmitted symbols with unit energy and r is the corresponding narrow-band radar signals.

The transmitted symbols x are digitally modulated to represent M possibilities, and its m-th possible baseband equivalent signal can be expressed by

$$x_m = I_m + jQ_m \tag{2}$$

$$= A_m e^{j\varphi_m} \tag{3}$$

$$A_m = \sqrt{I_m^2 + Q_m^2} \tag{4}$$

$$\varphi_m = \tan^{-1}\frac{I_m}{Q_m}, 1 \le m \le M, \tag{5}$$

where A_m and φ_m denote the amplitude and phase of the m-th possible signal, I_m and Q_m are the in-phase and quadrature

components of of the m-th possible signal. Then, its passband representation can be expressed as

$$\tilde{x}_m(t) = \Re[x_m e^{j2\pi f_c t}] \tag{6}$$
$$= \Re[A_m e^{j[2\pi f_c t + \varphi_m]}] \tag{7}$$
$$= A_m \cos[2\pi f_c t + \varphi_m], \tag{8}$$

where f_c denotes the carrier frequency. In this work, we consider two types of modulation schemes:

1) Phase shift keying (PSK): The signal phase $\varphi_m = \frac{2\pi}{M}(m-1)$, where $m = 1, 2, ..., M$, to represent $\log_2 M$ bits. When $M = 4$, the sinusoids represent symbol 00, 01, 11 or 10 with phase angles 0, $\frac{\pi}{2}$, π, $\frac{3\pi}{2}$ and a constant amplitude assuming $A_m = 1$ [28]. Additionally, the phase angles for QPSK can also be $\frac{\pi}{4}$, $\frac{3\pi}{4}$, $\frac{5\pi}{4}$ and $\frac{7\pi}{4}$.
2) Quadrature amplitude modulation (QAM): QAM changes both phases and amplitudes to represent $\log_2 M$ bits. For retangular 16QAM, $I_m = (2m-5)d$ and $Q_m = (2m-5)d$ for $1 \le m \le 4$ with $d = 1$, representing 4-digits symbols from 0000 to 1111. Moreover, the signal diagram can also be circular for different values of phases and amplitudes [28].

Linear frequency-modulation (LFM) and frequency-modulated continuous-wave (FMCW) are used as the interfering radar signal r. The baseband equivalent signal of a pulsed LFM radar waveform can be expressed as

$$r_{LFM}(t) = a(t)e^{j\phi(t)}, \tag{9}$$
$$\phi(t) = \frac{\pi\beta_1 t^2}{\tau_1}, \tag{10}$$
$$a(t) = \begin{cases} 1 & 0 \le t \le \tau_1 \\ 0 & \text{otherwise} \end{cases}, \tag{11}$$

where $\phi(t)$ denotes the instantaneous phase, $a(t)$ denotes the amplitude of the pulse waveform, β_1 is the signal bandwidth, τ_1 denotes the pulse duration. The baseband equivalent model of a FMCW radar $r_{FMCW}(t)$ can be expressed as

$$r_{FMCW}(t) = Ae^{j\theta(t)}, \tag{12}$$
$$\theta(t) = 2\pi \int_0^t \frac{\beta_2 x}{\tau_2}\, dx, \tag{13}$$

where A denotes the signal amplitude, β_2 is the signal bandwidth and τ_2 is the time duration.

In this paper, we will conduct experiments on detecting 16-ary quadrature amplitude modulation (16QAM) and quadrature phase shift keying (QPSK) signals in the presence of LFM and FMCW interference. The goal of this learning-based system is to recover the transmitted symbols from the received signals y directly without channel estimation and minimize the errors between the estimated symbols $\hat{x}$ and the transmitted symbols x in the presence of radar interference r, fading h and noise n.

III. Learning-based detection

The desired signals can be detected from the received signals by using neural networks with supervised learning. The structure of the learning-based detection is described in Fig.1. It is divided into two phases: training and deployment. In the training phase, we collect the transmitted symbols x and the corresponding received signals y corrupted by noise n and radar interference r. Note that the kth observed signal y_k is correctly matched with the kth transmitted symbol x_k. To let the machine recognize the transmitted symbol x_k, we model the detection process as a multi-classification problem and the kth symbol x_k can be represented by

$$\mathbf{s}_k = \begin{pmatrix} \Omega(x_k = c_1) \\ \Omega(x_k = c_2) \\ \cdots \\ \Omega(x_k = c_M) \end{pmatrix}, \tag{14}$$

where $\mathbf{s}_k$ is the one-hot representation of the transmitted symbol x_k, c_M denotes the constellation site of the transmitted symbols, $\Omega(.)$ is the encoding function that lets the symbol correspond to the element in the constellation be 1, and other elements be 0. The received signal training input for $\mathbf{s}_k$ as the training input can be expressed as

$$\mathbf{y}_k = \begin{pmatrix} y_k \\ y_{k-1} \\ y_{k-2} \\ \cdots \\ y_{k-l+1} \end{pmatrix}, 1 \le l \le k, \tag{15}$$

where $\mathbf{y}_k$ has a sequence of length l. Then, we label the training input $\mathbf{y}_k$ with the one-hot representation $\mathbf{s}_k$ of the corresponding transmitted symbol x_k to form the training dataset as

$$\{(\mathbf{s}_1, \mathbf{y}_1), (\mathbf{s}_2, \mathbf{y}_2), ..., (\mathbf{s}_k, \mathbf{y}_k)\}. \tag{16}$$

This dataset is utilized as the input to train the DNN detector that predicts the desired symbol x_k. Also, the features extracted from the observed signals can be added to the input of the neural network to help the training process. The outputs of the neural networks can be expressed as

$$\hat{\mathbf{s}}_k = f^m(f^{m-1}(\cdots f^1(\mathbf{y}_k, \beta)))), \tag{17}$$

where $\hat{\mathbf{s}}_k$ is the output prediction representing the estimation of the probability distribution of the transmitted symbol x_k; $f^m(.)$ denotes the mth layer of the neural network, β denotes the parameters of the network.

During the training, the optimal performance of the neural network is obtained by finding the optimized value of the parameter β in the network. First, the loss between the predicted symbol and the actual symbol is calculated through forward propagation. The categorical cross-entropy loss function is used for the multi-classification problem as

$$\mathcal{L} = -\sum_{k=1}^{M} \mathbf{s}_k \log \hat{\mathbf{s}}_k, \tag{18}$$

where $\mathbf{s}_k$ and $\hat{\mathbf{s}}_k$ are the actual labels and the outputs of the network, respectively. Then, gradient descend and back propagation algorithms are operated by feeding the training datasets to calculate the error and update the parameters of the network. To minimize the loss of each layer in the network, this iterative process continues until the loss cannot be reduced.

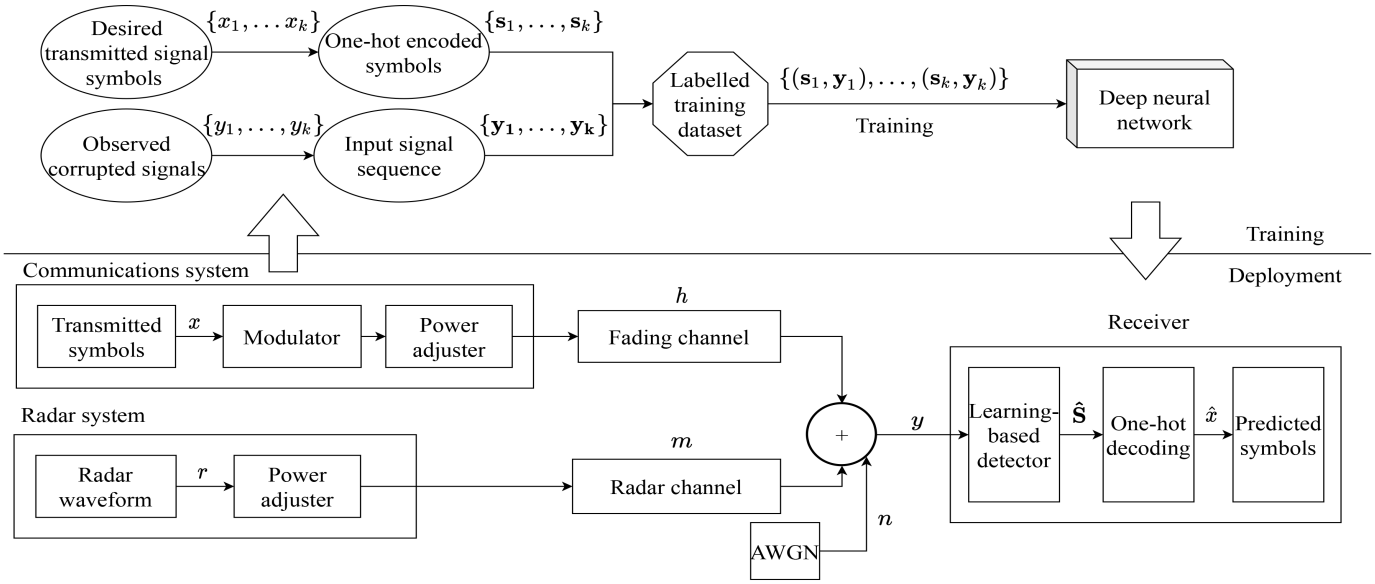

Fig. 1: The structure of learning-based detection.

In the deployment phase, the network is implemented at the receiver for detection. The output symbol representations $\hat{\mathbf{s}}_k$ are transformed to the predicted symbol $\hat{x}_k$. Note that the learning-based detection makes prediction by recognizing different patterns embedded in the signals and interference, and therefore, waveform design or interference mitigation is not required at the receiver.

A. FCDNN detector

FCDNN consists of several fully connected layers ending with a Softmax layer. Every neuron in the current layer takes the outputs of the previous layer as the input. The output of each fully connected layer can be expressed by

$$\mathbf{p}_m = \lambda(\mathbf{W}_m \mathbf{p}_{m-1} + \mathbf{b}_m), \tag{19}$$

where $\mathbf{p}_{m-1}$ is the output of the $(m-1)$-th layer of the fully connected neural network, $\mathbf{W}_m$ and $\mathbf{b}_m$ denote the weight and bias of the mth layer, respectively, λ is the activation function that introduces nonlinearity to the network. ReLU [29] and Softmax [30] are used in FCDNN. ReLU function can increase sparsity in the network by making a part of neurons, which reduces the interdependence of parameters and alleviate overfitting problems. Also, ReLU can effectively prevent gradient vanishing problem by maintaining a certain slope when the network is close to convergence. Softmax is used for the final layer, which outputs a probability mass function for the multi-classification problem.

B. LSTM detector

Recurrent neural networks (RNN) is applied mainly for sequence prediction in natural language processing and time series data processing. Long short-term memory (LSTM) is used as the RNN to reduce the long-term dependencies to the sequence. A LSTM layer can be described by

$$\mathbf{f}_t = \sigma_g(\mathbf{W}_f \mathbf{x}_t + \mathbf{U}_f \mathbf{h}_{t-1} + \mathbf{b}_f), \tag{20}$$

$$\mathbf{i}_t = \sigma_g(\mathbf{W}_i \mathbf{x}_t + \mathbf{U}_i \mathbf{h}_{t-1} + \mathbf{b}_i), \tag{21}$$

$$\mathbf{o}_t = \sigma_g(\mathbf{W}_o \mathbf{x}_t + \mathbf{U}_o \mathbf{h}_{t-1} + \mathbf{b}_o), \tag{22}$$

$$\mathbf{C}_t = \mathbf{f}_m \mathbf{C}_{t-1} + \mathbf{i}_m \tanh(\mathbf{W}_c \mathbf{h}_t + \mathbf{U}_c \mathbf{h}_{t-1} + \mathbf{b}_c), \tag{23}$$

$$\mathbf{h}_t = \mathbf{o}_t \tanh(\mathbf{C}_t) \tag{24}$$

where $\mathbf{f}_t$, $\mathbf{i}_t$, $\mathbf{o}_t$, $\mathbf{C}_t$ and $\mathbf{h}_t$ denote the forget gate, the input gate, the output gate, the cell state and the layer output; $\mathbf{W}$, $\mathbf{U}$ and $\mathbf{b}$ are the weights and bias in the model; σ_g denote the gate activation function which is normally the sigmoid function. The current layer output $\mathbf{h}_t$ can be calculated by above equations with the input $\mathbf{x}_t$ and previous state $\mathbf{h}_{t-1}$. RNN can be used to cope with time series data by considering data information in the previous time period. In this case, the observations from the previous symbols are concluded as the states for predicting the current symbol. Unlike the symbol-by-symbol detector FCDNN, RNN makes predictions by learning from a sequence of symbols and recover a sequence of symbols. In this paper, we use LSTM as the sequence detector which is improved from traditional RNN by reducing the long-term dependencies, gradient vanishing and exploding.

C. Interference at communication

In a traditional wireless communications system, interference is commonly mitigated by filters according to their different characteristics from the transmitted signals, such as frequency. Unlike the traditional communication system, DNN signal detector directly recovers signals at the receiver from the corrupted signals by recognizing the patterns without filtering. This process is modeled as a multi-classification problem. Therefore, a DNN signal detector does not require interference mitigator at receiver. This simplifies the system design. Previous works have proved the feasibility of using

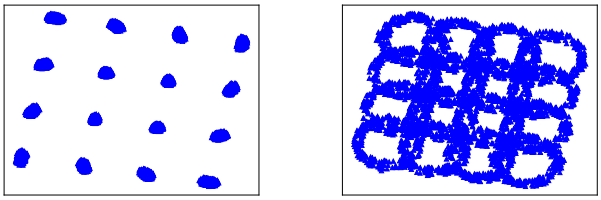

(a) (b)

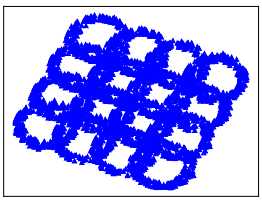

(c)

Fig. 2: Constellations of 16QAM signals in the presence of radar interference (a) SIR = 30 dB (b) SIR = 10 dB (c) SIR = 10 dB with preprocessing by PCA.

deep neural network to solve the signal detection problem and most of these works focused on how signal detection benefits from the different structures of neural networks. However, the detection accuracy encounters a bottleneck in the presence of interference when the raw data is used as the input to the network. Fig. 2 shows the 16QAM signals with different signal-to-interference ratios of radar interference. It can be observed that different symbols maintain a clear distance from each other when SIR is 30 dB in Fig. 2(a), which can be classified easily by their coordinates in the constellation diagram. However, when SIR is 10 dB in Fig. 2(b), the adjacent symbols start to intersect. Therefore, different symbols may have similar coordinates on the constellation. Consequently, it is difficult for the neural network to identify different symbols with similar data input. Also, this problem cannot be solved by improving the structure of the network since we have to consider the tradeoff between overfitting and identifying symbols. Therefore, preprocessing the datasets becomes necessary to improve the detection performance.

D. Data preprocessing

Data preprocessing has been widely utilized in machine learning, such as data quality assessment, feature aggregation, dimensionality reduction and feature extraction. Data preprocessing is a process to transform the data so that machines can efficiently parse it to improve the performance. In this paper, the input to the network is the observed signals or their features. Each observed complex-value symbol can be considered as a two-dimensional coordinate on the constellation diagram. To make different symbols less intersect on the constellation, we use principal component analysis (PCA) to preprocess the datasets. PCA is often considered as an unsupervised learning method for dimensionality reduction. However, we use PCA to generate new features from the observed symbols. As shown in Fig. 2(c), the constellation diagram is rotated with a certain angle by PCA compared with Fig. 2(b). PCA can learn the best rotation angle based on the density of points in the original coordinate system and convert these points into the same space to obtain higher accuracy. Mathematically, PCA is based on orthogonal transformation and the values of the transformed data are the scalar projection of the original coordinates.

IV. Simulation environment

The simulation environment of this work is implemented using Matlab and the key components are shown below:

1) Input bitstream: A binary bitstream is generated randomly as the input information of the signal transmitter.
2) Digital modulator: The binary information in the communications system is modulated to complex-value I/Q signals. 16QAM and QPSK modulation schemes are used as the modulators in the simulation.
3) Radar waveform: LFM and FMCW signals are generated as the radar interference.
4) Channel: Rician fading channel is applied for communication system to describe a line-of-sight radio propagation. LOS channel is also modeled for radar waveforms with the attenuation due to the atmospheric parameters.
5) AWGN: The thermal noise at the receiver is described by additive white Gaussian noise and its variance is applied to model the noise power.
6) Transmitter: Power adjuster is implemented to control the signal-to-interference ratio and signal-to-noise ratio.
7) Receiver: Both LSTM and FCDNN based signal detectors are deployed at the receiver to detect the signals, while the traditional detector with least-squares channel estimation and zero-forcing detection is deployed as a benchmark.

The signal-to-interference ratio (SIR) is defined by

$$SIR = 10\lg\frac{P_s}{P_r}, \tag{25}$$

where P_s denotes the average power of the transmitted signal in the communications system, which is normalized as unit in the simulation; P_r denotes the average power of the interference radar signals. The signal-to-noise ratio (SNR) is determined by

$$SNR = 10\lg\frac{P_s}{P_n}, \tag{26}$$

where P_n denotes the noise power which specifies the variance of the AWGN. In the simulation, SIR and SNR are measured at the receiver and the signal intensity is adjusted at transmitter.

The parameters setting for the learning-based detectors are given in Table I. We use open-source Keras and TensorFlow as the backend to implement FCDNN and LSTM. Adam optimizer is applied and the learning rate is set at 0.001. To prevent overfitting, we use early stopping techniques during training.

TABLE I: Parameters of learning-based detector

	LSTM	FCDNN
Batch size	32	512
Learning rate	0.001	0.001
Training epochs	100	150
Number of LSTM layers	2	-
Number of fully connected layers	1	10
Sequence length	20	1

V. Numerical Results and Discussion

In this section, numerical results are presented to evaluate the performances of the learning-based detectors in the presence of radar interference. Note that we use the signals for all SNR and SIR values to train the model and then we test our model in different SNRs and SIRs. Firstly, we compare the performance for different numbers of layers and features for the FCDNN detector. Then, we compare the performance of FCDNN, LSTM and the zero-forcing detectors with varying SIRs. Afterwards, we investigate the effects of interference coverage represented by different pulse widths of LFM. Finally, we consider the effect of symbol duration of the transmitted signals.

A. Effects of features and layers for FCDNN

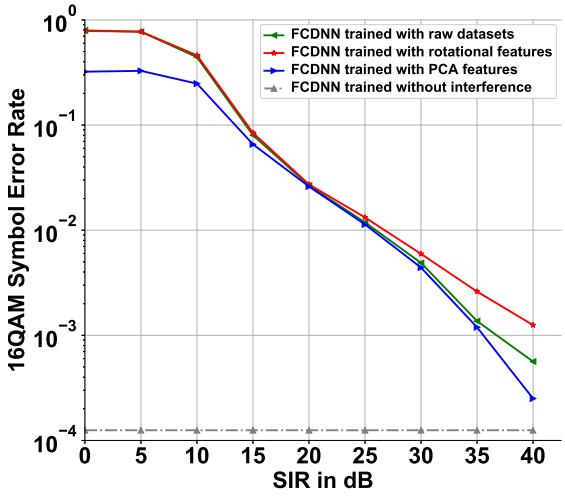

Fig. 3: Symbol error rate of 16QAM signals with detectors having different features when the SNR is 40 dB.

To improve the accuracy of FCDNN symbol-by-symbol detector, feature extraction is utilized to find a better representation for the raw datasets as the input to the network. Each complex-value received signal can be considered as a two-dimensional coordinate on the constellation, and we transform the coordinates to rotational coordinates to add more feature information. PCA is applied to learn the best rotational angle and transform the data into the same space in order to obtain higher accuracy. We evaluate the performance for varying SIRs from 0 to 40 dB with a step size of 5 dB and we take the SER performance of FCDNN in the absence of interference as the benchmark.

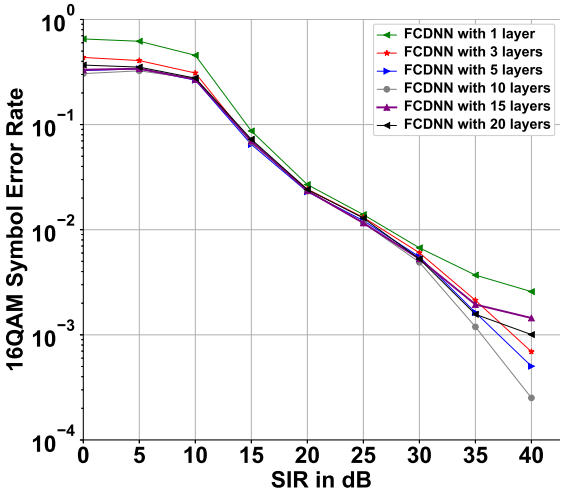

Fig. 4: Symbol error rate of 16QAM signals with detectors having different layers when the SNR is 40 dB.

Fig. 3 compares the performance of the detector with different feature transformation methods. The SER performance without interference remains the lowest at about 1.2×10^{-4} as it is not affected by SIR. One sees that FCDNN with features preprocessed by PCA has better performance than the detectors trained by raw datasets or manual rotation features. When SIR is less than 15 dB, FCDNN trained by raw datasets achieves similar accuracy to FCDNN trained by rotation features while FCDNN trained by PCA outperforms them by approximately 40% in SER, although the gap reduces as SIR increases. This is because PCA transformation reduces the intersection on the constellation caused by interference and noise, which simplifies the classification for the detector. When SIR is beyond 30 dB, FCDNN trained by raw datasets outperforms FCDNN trained by rotational features, while FCDNN trained by PCA has the lowest SER among the 3 FCDNN detectors. This shows that PCA preprocessing improves the performance in the conditions of very low SIRs and very high SIRs.

On the other hand, the classification capacity of neural networks can be improved by simply increasing the number of hidden layers, but too many hidden layers can cause overfitting and consequently degrade the system performance. Therefore, we conducted experiments to discover how the system performance changes with the increase of layers. We consider the system of detecting 16QAM signals under LFM interference for SIR from 0 to 40 dB with a step size of 5 dB. In Fig. 4, the performance of FCDNN detector for different numbers of hidden layers is evaluated. FCDNN with ten layers achieves the best performance while FCDNN with one layer has the highest SER due to the lack of learning ability. When SIR is less than 20 dB, the performance of the detector improves as the number of layers increases although the performance gap narrows as the SIR grows. When SIR reaches 40 dB, FCDNN

with ten layers remains the lowest SER while FCDNN with 15 and 20 layers outperforms FCDNN with one layer. This shows that increasing layers can improve the learning ability for recognizing highly corrupted signals. However, having over ten layers can cause overfitting problems and affect the performance in high SIR conditions.

B. Effect of varying SIRs

In this section, we compare the SER performance with respect to the SIRs of the radar-communication system. To simulate the performance, SIR are set from 0 to 40 dB with a step size of 5 dB and randomly generated sequences of 32000 bits are utilized as the input stream. LFM waveform with pulse width 10^{-3} seconds and pulse repetition frequency 10^3 Hz is simulated as the radar interference. A suboptimal zero-forcing detector with pilot-aided least-squares channel estimation is implemented as the benchmark. Sequence detector LSTM and symbol-by-symbol detector FCDNN with PCA are implemented for comparison.

Fig. 5(a) compares the performance when the SNR is 40 dB to simulate the situation where there is weak noise. The SER of FCDNN ranges from about 3×10^{-1} to $2\times10-4$ when the SIR increases from 0 to 40 dB while the SER of LSTM decreases from about 8×10^{-1} to 1.5×10^{-4}. When SIR is less than 15 dB, FCDNN can outperform other detectors while the sequence detector LSTM can achieve similar performance to the zero-forcing detector. This proves that FCDNN trained with PCA can improve the performance when SIR is low, compared with the zero-forcing detector and LSTM sequence detector. As the SIR goes beyond 15 dB, the SER of FCDNN becomes lower than other detectors and mixes with the SER of the zero-forcing detector. Also, the sequence detector LSTM starts to outperform others until SIR reaches 40 dB. This is because PCA cannot effectively reduce the intersection between symbols when the SIR condition is relatively good while sequence detector and traditional detector can handle the channel distortions by training with a sequence of symbols or having pilot-aided channel estimation.

Fig. 5(b) evaluates the performance when the SNR is 0 dB to simulate the strong noise. In Fig. 5(b), both FCDNN and LSTM outperform the zero-forcing detector with the least-squares channel estimation, while LSTM is slightly better than FCDNN when SIR is beyond 10 dB. FCDNN and LSTM can achieve the best performance of 7×10^{-2} and 6×10^{-2} SER, while the zero-forcing detector can only achieve about 2×10^{-1} and 4×10^{-1} SER when the pilot interval is 10 and 100 symbols, respectively. Least-squares channel estimation may aggravate the influence of noise in the case of low SNR for the zero-forcing detectors, but it also proves that the learning-based detector can reduce performance degradation when the channel is highly corrupted by noise. Also, LSTM takes a sequence of symbols into consideration in the estimation of one symbol by memorizing the state of the previous symbols. This enables LSTM to know the hidden connections between symbols. On the other hand, FCDNN learns the symbols distributions in the constellations but cannot overcome the time-related channel distortions.

We also conducted experiments to detect QPSK signals in the presence of LFM interference. In Fig. 6(a), LSTM and FCDNN outperform the zero-forcing detector because the learning-based detector can benefit from the increased Euclidean distance of QPSK symbols. Specifically, the SER of LSTM and FCDNN decreases from about 7×10^{-2} and 1.5×10^{-1} to 10^{-3} when SIR grows from 0 to 5 dB, while the zero-forcing detector requires about 4 dB more to achieve similar performances. In Fig. 6(b), the learning-based detector can achieve about 10^{-3} at a SIR of 10 dB while the zero-forcing detector can only achieve about 1.4×10^{-1}. Also, when the SNR is 10 dB, the performance gap between the zero-forcing detector and the learning-based detector increases as the SIR grows and the SER of the learning-based reduces much faster than the zero-forcing detector.

C. Effect of FMCW interference

In this section, we evaluate the performance of detecting 16QAM signals in the presence of FMCW interference. Fig. 7 describes the SER performance when the SNR is 40 dB and 10 dB to simulate different levels of noise corruption. In Fig. 7(a), LSTM and FCDNN have better SER performance than the zero-forcing detector when SIR is less than 25 dB while the zero-forcing detector slightly outperforms the learning-based detectors when SIR is over 35 dB. To explain this, LSTM and FCDNN are trained by the datasets with signals for SIR from 0 to 40 dB with a step size of 5 dB. In order to optimize the overall performance across all the SIR conditions, the training may make compromisation between the performance in the low SIR range and the performance in the high SIR range. In this case, the learning-based model sacrificed a bit accuracy in the high SIR range to obtain a better overall accuracy so that they are worse than the ZF detectors in the high SIR range. Numerically, the SER of LSTM and FCDNN ranges from about 5.5×10^{-1} to 2×10^{-3} when SIR grows from 0 to 40 dB, which is slightly higher than those in the presence of LFM interference in Section V-B. This shows that FMCW degrades the performance more under the same SIR, because the continuous wave of FMCW occupies a longer time than the pulsed wave of LFM. To prove this, we will evaluate the performance of different interference coverage in the next section. In Fig. 7(b), LSTM and FCDNN outperform the zero-forcing detector, similar to the results in Section V-B. This shows that LSTM and FCDNN can achieve good performance when SNR is low.

D. Effect of interference coverage

In this section, we evaluate the performances of the learning-based detectors with respect to different interference coverage. The continuous wave has full interference coverage on the transmitted communications signals while pulsed wave has a periodic interference zone depending on the pulse width and pulse repetition frequency. Therefore, We describe the interference coverage by the pulse width of LFM interference, which specifies the length of each pulse in seconds. We consider the pulse width from 10^{-4} to 10^{-3} seconds with a step size of 10^{-4} seconds and pulse repetition frequency 10^3

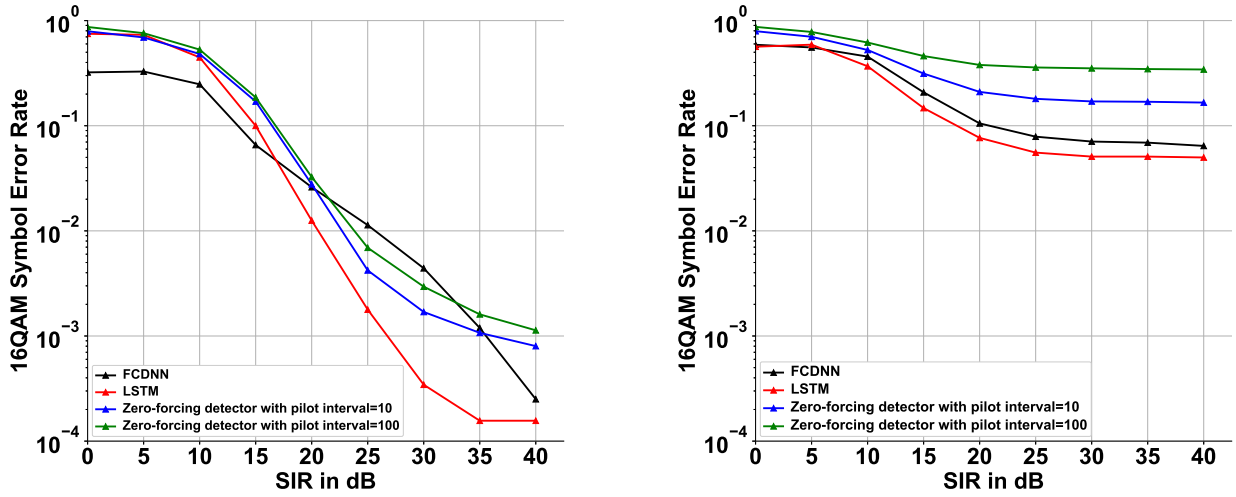

(a) (b)

Fig. 5: Symbol error rate of 16QAM signals in the presence of LFM interference. (a) The performance when the SNR is 40 dB. (b) The performance when the SNR is 10 dB.

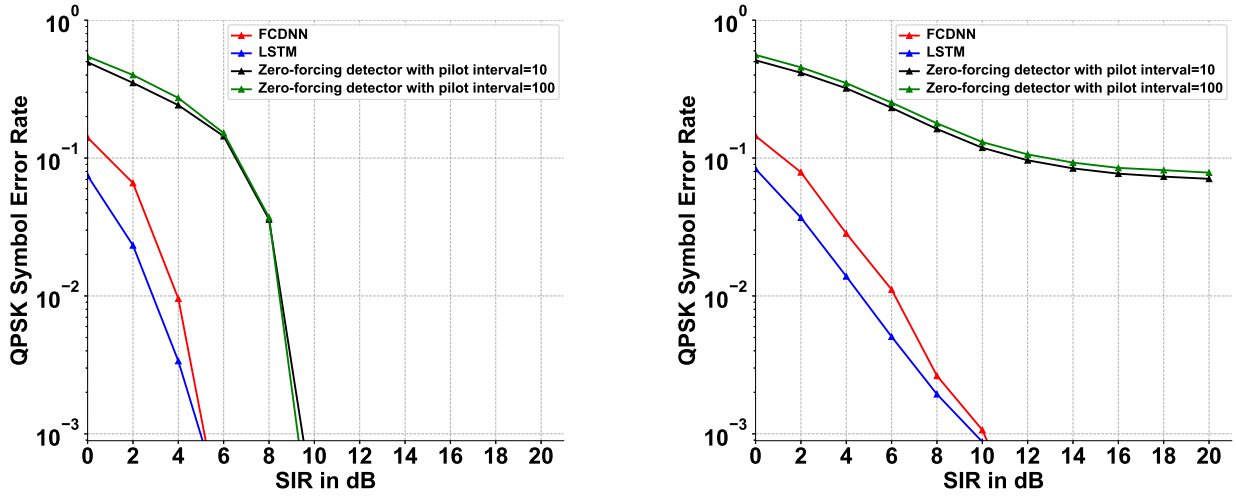

(a) (b)

Fig. 6: Symbol error rate of QPSK signals in the presence of LFM interference. (a) The performance when SNR is 40 dB. (b) The performance when SNR is 10 dB.

Hz. Also, we set SIR=0 dB and SIR=30 dB to describe the strongly interfered and weakly interfered cases.

Fig. 8 compares the SER for 16QAM signals in the presence of LFM interference with different pulse widths. Interestingly, we can observe that the SER increases as the pulse width increases. This is because there is no interference during the time interval between adjacent radar pulses and the longer pulse width causes more interference coverage for fixed pulse repetition frequency. Although the longer pulse width also reduces the peak amplitude of the radar interference for the same SIR, the results indicate that radar interference coverage can have a greater impact on performance than the peak amplitude of interference. Also, FCDNN outperforms LSTM when SIR is 0 dB, while LSTM has better performance when SIR is 30 dB. Specifically, the SER performance of FCDNN increases from 4×10^{-2} to 3×10^{-1} when the pulse width increases and the SIR is 0, while the SER performance of LSTM ranges from about 9×10^{-2} to 7×10^{-1}. When SIR is 30 dB, the SER of LSTM increases from about 2×10^{-4} to 1.5×10^{-3} while the SER of FCDNN ranges from 8×10^{-4} to 5×10^{-3}.

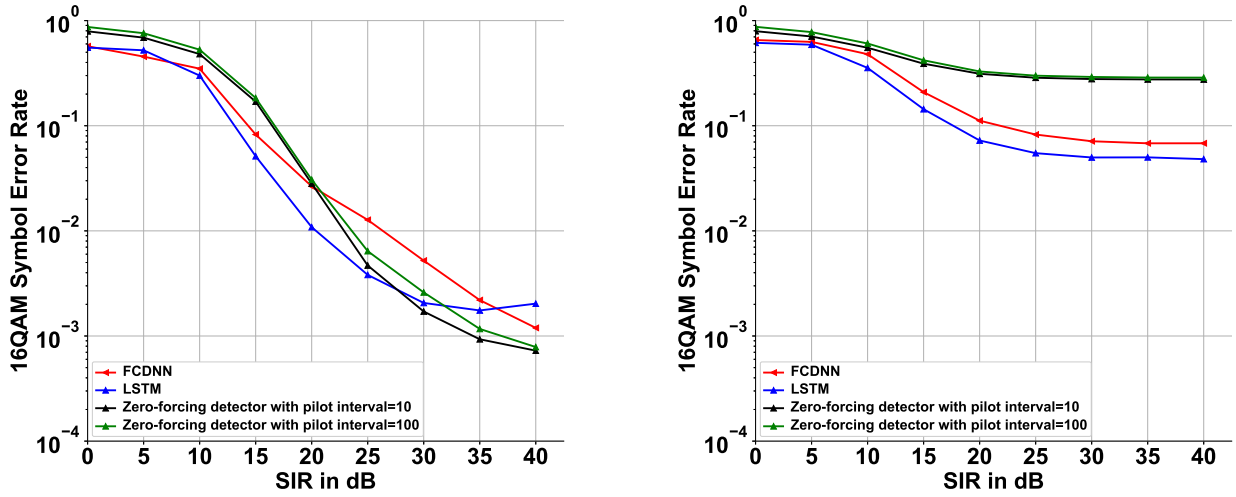

(a) (b)

Fig. 7: Symbol error rate of 16QAM signals in the presence of FMCW interference. (a) The performance when the SNR is 40 dB. (b) The performance when the SNR is 10 dB.

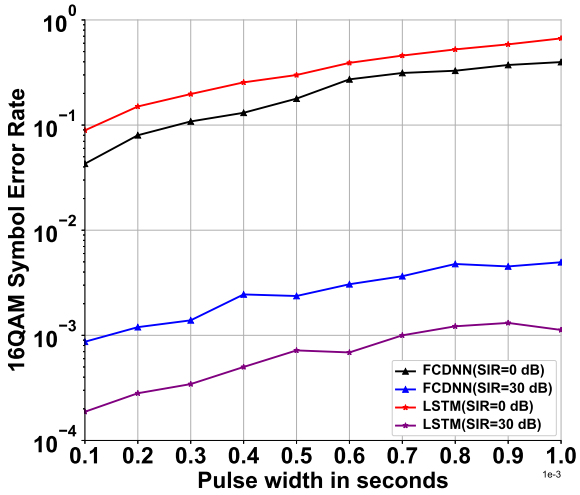

Fig. 8: Symbol error rate of 16QAM signals in the presence of LFM interference with different pulse widths when the SNR is 40 dB.

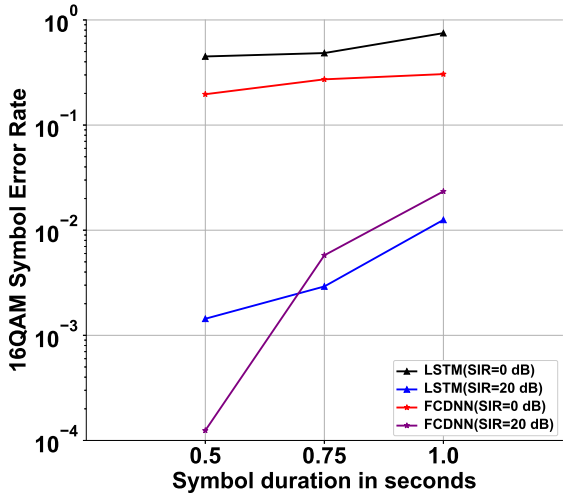

Fig. 9: Symbol error rate of 16QAM signals with detectors having different symbol duration when the SNR is 40 dB.

E. Effect of symbol duration

In general, increasing the number of training samples improves the classification of the detector. In a communications system, this takes more time to receive the signals and introduces more time-related distortions on signals. Therefore, we conducted experiments to study how the symbol duration affects the detection performance. Fig. 9 shows the performance of detecting 16QAM signals with a symbol duration of 0.5, 0.75 and 1.0 seconds, which means we collected 16000, 24000 and 32000 symbols for training at a 32000 Hz sample rate.

In this figure, the SER of FCDNN and LSTM increases as the symbol duration increases. Also, FCDNN outperforms LSTM at 20 dB SIR for a symbol duration of 0.5 seconds, which is different from those at 0.75 and 1.0 seconds. To show why FCDNN performs differently from LSTM at 20 dB SIR, Fig. 10 shows the 16QAM constellations with a symbol duration of 0.5, 0.75 and 1.0 seconds when SIR is 20 dB. One sees that, as the symbol duration increases, signals on constellation appear clockwise distortion and offset. The distortion is mainly caused by Doppler shift. This distortion blurs the boundaries of different symbols and causes difficulties especially to FCDNN detector for classification as it only takes features of the current symbol without considering the previous symbols. Therefore, LSTM can outperform FCDNN when the symbol duration

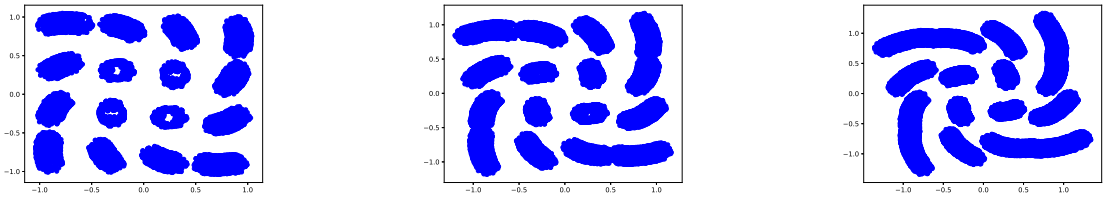

(a) (b) (c)

Fig. 10: Constellations of 16QAM signals with different symbol duration when the SIR = 20 dB and the SNR = 40 dB. (a) The constellation when symbol duration is 0.5 seconds. (b) The constellation when symbol duration is 0.75 seconds. (c) The constellation when symbol duration is 1.0 second.

increases, while FCDNN has high accuracy when the symbol duration is short and the boundaries of different symbols are clear.

VI. Conclusion

In this paper, we have proposed the learning-based signal detection scheme for the co-existing radar-communication system using FCDNN and LSTM. LFM and FMCW have been studied as interference to the communications system. Performance of the learning-based detector has been compared under several scenarios, including intensity of interference and noise, layers of the networks and symbol duration. Numerical results have shown that the learning-based detector achieves better performance than the zero-forcing detector for 16QAM and QPSK signals in varied SIRs and SNRs. In addition, the simulation results have proven that preprocessing the complex-value observed signals with the PCA algorithm improves the system performance of the FCDNN detector. Also, increasing layers improves the performance of the FCDNN detector in the low-SIR conditions but beyond a certain number of layers may cause overfitting and consequently compromise the accuracy when SIR is high. However, the performance of FCDNN can be affected more by time-related distortion than LSTM. Furthermore, for the same SIR, the communications system can be degraded more by the more extensive interference coverage than the higher peak amplitude of the radar interference.

References

[1] C. Shi, F. Wang, M. Sellathurai, J. Zhou, and S. Salous, "Power minimization-based robust ofdm radar waveform design for radar and communication systems in coexistence," *IEEE Transactions on Signal Processing*, vol. 66, no. 5, pp. 1316–1330, March 2018.

[2] M. Bică and V. Koivunen, "Radar waveform optimization for target parameter estimation in cooperative radar-communications systems," *IEEE Transactions on Aerospace and Electronic Systems*, vol. 55, no. 5, pp. 2314–2326, Oct 2019.

[3] X. Wang, A. Hassanien, and M. G. Amin, "Dual-function mimo radar communications system design via sparse array optimization," *IEEE Transactions on Aerospace and Electronic Systems*, vol. 55, no. 3, pp. 1213–1226, June 2019.

[4] S. Zhou, X. Liang, Y. Yu, and H. Liu, "Joint radar-communications co-use waveform design using optimized phase perturbation," *IEEE Transactions on Aerospace and Electronic Systems*, vol. 55, no. 3, pp. 1227–1240, June 2019.

[5] H. Deng and B. Himed, "Interference mitigation processing for spectrum-sharing between radar and wireless communications systems," *IEEE Transactions on Aerospace and Electronic Systems*, vol. 49, no. 3, pp. 1911–1919, July 2013.

[6] L. Zheng, M. Lops, and X. Wang, "Adaptive interference removal for uncoordinated radar/communication coexistence," *IEEE Journal of Selected Topics in Signal Processing*, vol. 12, no. 1, pp. 45–60, Feb 2018.

[7] F. Liu, C. Masouros, A. Li, T. Ratnarajah, and J. Zhou, "Mimo radar and cellular coexistence: A power-efficient approach enabled by interference exploitation," *IEEE Transactions on Signal Processing*, vol. 66, no. 14, pp. 3681–3695, July 2018.

[8] H. Shajaiah, A. Khawar, A. Abdel-Hadi, and T. C. Clancy, "Resource allocation with carrier aggregation in lte advanced cellular system sharing spectrum with s-band radar," in *2014 IEEE International Symposium on Dynamic Spectrum Access Networks (DYSPAN)*, April 2014, pp. 34–37.

[9] N. Nartasilpa, A. Salim, D. Tuninetti, and N. Devroye, "Communications system performance and design in the presence of radar interference," *IEEE Transactions on Communications*, vol. 66, no. 9, pp. 4170–4185, Sep. 2018.

[10] L. Zheng, M. Lops, X. Wang, and E. Grossi, "Joint design of overlaid communication systems and pulsed radars," *IEEE Transactions on Signal Processing*, vol. 66, no. 1, pp. 139–154, Jan 2018.

[11] A. D. Harper, J. T. Reed, J. L. Odom, A. D. Lanterman, and X. Ma, "Performance of a linear-detector joint radar-communication system in doubly selective channels," *IEEE Transactions on Aerospace and Electronic Systems*, vol. 53, no. 2, pp. 703–715, April 2017.

[12] F. Wang, H. Li, and M. A. Govoni, "Power allocation and co-design of multicarrier communication and radar systems for spectral coexistence," *IEEE Transactions on Signal Processing*, vol. 67, no. 14, pp. 3818–3831, July 2019.

[13] E. Grossi, M. Lops, and L. Venturino, "Joint design of surveillance radar and mimo communication in cluttered environments," *IEEE Transactions on Signal Processing*, vol. 68, pp. 1544–1557, 2020.

[14] D. Cohen, K. V. Mishra, and Y. C. Eldar, "Spectrum sharing radar: Coexistence via xampling," *IEEE Transactions on Aerospace and Electronic Systems*, vol. 54, no. 3, pp. 1279–1296, June 2018.

[15] A. Krizhevsky, I. Sutskever, and G. E. Hinton, "Imagenet classification with deep convolutional neural networks," *Commun. ACM*, vol. 60, no. 6, p. 84–90, May 2017. [Online]. Available: https://doi.org/10.1145/3065386

[16] K. Cho, B. van Merrienboer, C. Gulcehre, D. Bahdanau, F. Bougares, H. Schwenk, and Y. Bengio, "Learning Phrase Representations using RNN Encoder-Decoder for Statistical Machine Translation," *arXiv e-prints*, p. arXiv:1406.1078, Jun. 2014.

[17] T. O'Shea and J. Hoydis, "An introduction to deep learning for the physical layer," *IEEE Transactions on Cognitive Communications and Networking*, vol. 3, no. 4, Dec 2017.

[18] D. Gündüz, P. de Kerret, N. D. Sidiropoulos, D. Gesbert, C. R. Murthy, and M. van der Schaar, "Machine learning in the air," *IEEE Journal on Selected Areas in Communications*, vol. 37, no. 10, pp. 2184–2199, Oct 2019.

[19] N. Samuel, T. Diskin, and A. Wiesel, "Deep mimo detection," in *2017 IEEE 18th International Workshop on Signal Processing Advances in Wireless Communications (SPAWC)*, July 2017, pp. 1–5.

[20] M. Baek, S. Kwak, J. Jung, H. M. Kim, and D. Choi, "Implementation methodologies of deep learning-based signal detection for conventional mimo transmitters," *IEEE Transactions on Broadcasting*, vol. 65, no. 3, pp. 636–642, Sep. 2019.

[21] H. Ye, G. Y. Li, and B. Juang, "Power of deep learning for channel

estimation and signal detection in ofdm systems," *IEEE Wireless Communications Letters*, vol. 7, no. 1, pp. 114–117, Feb 2018.
[22] N. Farsad and A. Goldsmith, "Neural network detection of data sequences in communication systems," *IEEE Transactions on Signal Processing*, vol. 66, no. 21, pp. 5663–5678, Nov 2018.
[23] N. Shlezinger, N. Farsad, Y. C. Eldar, and A. J. Goldsmith, "Viterbinet: A deep learning based viterbi algorithm for symbol detection," *IEEE Transactions on Wireless Communications*, vol. 19, no. 5, pp. 3319–3331, May 2020.
[24] H. He, C. Wen, S. Jin, and G. Y. Li, "A model-driven deep learning network for mimo detection," in *2018 IEEE Global Conference on Signal and Information Processing (GlobalSIP)*, Nov 2018, pp. 584–588.
[25] H. He, C. Wen, S. Jin, and G. Y. Li, "Model-driven deep learning for mimo detection," *IEEE Transactions on Signal Processing*, vol. 68, pp. 1702–1715, 2020.
[26] X. Jin and H. Kim, "Parallel deep learning detection network in the mimo channel," *IEEE Communications Letters*, vol. 24, no. 1, pp. 126–130, Jan 2020.
[27] C. Liu, Y. Chen, and S.-H. Yang, "Signal detection with co-channel interference using deep learning," *Physical Communication*, vol. 47, p. 101343, 2021.
[28] J. G. Proakis and M. Salehi, *Digital Communications*. Boston: McGraw-Hill, 2008.
[29] A. F. Agarap, "Deep Learning using Rectified Linear Units (ReLU)," *arXiv e-prints*, p. arXiv:1803.08375, Mar. 2018.
[30] C. Nwankpa, W. Ijomah, A. Gachagan, and S. Marshall, "Activation Functions: Comparison of trends in Practice and Research for Deep Learning," *arXiv e-prints*, p. arXiv:1811.03378, Nov. 2018.

Chenguang Liu Chenguang Liu received his B.E. degree in software engineering from Dalian University of Technology, Dalian, P.R.China, in 2016 and M.S. degree in advanced computer science from The University of Manchester, U.K., in 2017. He is currently studying as a Ph.D. student at the University of Warwick, U.K. His research interests include deep learning, wireless communications and signal detection.

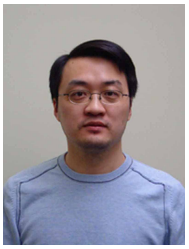

Yunfei Chen Yunfei Chen (S'02-M'06-SM'10) received his B.E.and M.E. degrees in electronics engineering from Shanghai Jiaotong University, Shanghai, P.R.China,in 1998 and 2001, respectively. He received his Ph.D. degree from the University of Alberta in 2006. He is currently working as an Associate Professor at the University of Warwick, U.K. His research interests include wireless communications, cognitive radios, wireless relaying and energy harvesting.

Shuang-Hua Yang Shuang-Hua YANG received the B.S. degree in instrument and automation and the M.S. degree in process control from the China University of Petroleum (Huadong), Beijing, China, in 1983 and 1986, respectively, and the Ph.D. degree in intelligent systems from Zhejiang University, Hangzhou, China, in 1991. He was awarded DSc from Loughborough University in 2014 to recognize his academic contribution to wireless monitoring research. He is currently a chair professor of computer science and vice dean of graduate school with Southern University of Science and Technology (SUSTech), Shenzhen, China. Before joined SUSTech in 2016 he had spent over two decades in Loughborough University, as a professor in computer science and head of department. His current research interests include cyber-physical system safety and security, Internet of Things, wireless network-based monitoring and control. He is a Fellow of IET and a Fellow of InstMC, U.K. He is an Associate Editor of the IET Journal Cyber-Physical Systems Theory and applications and the InstMC Journal Measurement and Control.